Supplementary Information for the manuscript titled "Electrophoretic motion of a non-uniformly charged particle in a viscoelastic medium in thin electrical double layer limit"

Uddipta Ghosh[1], Siddhartha Mukherjee[2], and Suman Chakraborty[2,3]

[1]*Department of Mechanical Engineering, Indian Institute of Technology Gandhinagar, Palaj - 382355, Gujrat, India*
[2]*Advanced Technology Development Centre, Indian Institute of Technology Kharagpur, Kharagpur - 731302, West Bengal, India*
[3]*Department of Mechanical Engineering, Indian Institute of Technology Kharagpur, Kharagpur - 731302, West Bengal, India*

This supplementary information document is divided into four distinct sections. In §S1, we provide a detailed derivation of the *Modified Smoluchowski Slip Velocity* at $\mathcal{O}(\bar{\zeta}_0^3)$ in a viscoelastc medium, by taking into consideration particle's rotation. This section complements §3 and of the main manuscript and in particular eqn. (3.20) therein. In §S2, we complement §4.2 of the main manuscript; here we outline the expressions for the stream functions and their components at $\mathcal{O}(\bar{\zeta}_0^3)$. In §S3, additional details on the numerical simulations for FENE-P constitutive model discussed in §4.4 of the main manuscript have been included. Finally, §S4 is dedicated to provide further insights into the distribution of polymeric stresses around the particle, in the outer layer. This section complements the discussions on "*birefringent strands*" in §4.5 of the main manuscript.

S1 Derivation of Modified Smoluchowski Slip with particle rotation

S1.1 Assumptions associated with particle rotation

It is assumed that the particle rotates with angular velocity $\mathbf{\Omega}$ around it's center. In general, this angular velocity may be expressed as: $\mathbf{\Omega} = \Omega_x\hat{\mathbf{e}}_x + \Omega_y\hat{\mathbf{e}}_y + \Omega_z\hat{\mathbf{e}}_z$. Because of rotation, the charge distribution on the particle surface with respect to a frame fixed at the particle's center (but not rotating with the particle) will change with time, which naturally makes the flow unsteady. However, the analysis simplifies if the time scale of rotation ($|\mathbf{\Omega}|^{-1}$) is large as compared to the relaxation and retardation time scales of the fluid. We therefore assume that $|\mathbf{\Omega}|^{-1} \gg \lambda_1',\ \lambda_2'$ is satisfied, which ensures that the motion is quasi-steady and the flow field around the particle depends on the instantaneous angular and translational velocity of the same. It is clear that the above condition is satisfied for slow rotation of the particle. To

complete the description, it is necessary to determine how the surface charge density evolves in time, so that it is a known quantity at any given time. The rate of change of surface charge density is given by:

$$\frac{\partial \zeta}{\partial t} = \frac{\partial \zeta}{\partial \theta}\dot{\theta} + \frac{\partial \zeta}{\partial \varphi}\dot{\varphi} \tag{S1}$$

It may be verified that the rate of change of angles θ and φ of a point on the particle surface is linked to it's angular velocity as follows:

$$\dot{\theta} = (\boldsymbol{\Omega} \times \hat{\mathbf{e}}_r) \cdot \hat{\mathbf{e}}_\theta = \Omega_y \cos\varphi - \Omega_x \sin\varphi \tag{S2a}$$

$$\text{and } \dot{\varphi} = (\boldsymbol{\Omega} \times \hat{\mathbf{e}}_r) \cdot \hat{\mathbf{e}}_\varphi = -\left[\Omega_y \sin\varphi + \Omega_x \cos\varphi\right]\cos\theta + \Omega_z \sin\theta \tag{S2b}$$

Once the angular velocities are known, eqn. (S1) may be solved to deduce the surface charge distribution at the subsequent times, subject to some pre-specified initial condition.

S1.2 The leading order Salt and Current flux matching conditions

Eqn. (3.8) of the main manuscript outlines the leading order salt and current flux matching conditions at the edge of the EDL. These conditions are required to write solutions for the potential and the salt concentration in the outer layer. In this subsection, we present a brief derivation of the conditions mentioned in (3.8) of the manuscript. We can arrive at the necessary matching conditions by writing the Nernst-Plank equations in the following conservative form: $\boldsymbol{\nabla} \cdot \mathbf{i} = \boldsymbol{\nabla} \cdot \mathbf{j} = 0$, where $\mathbf{i}$ and $\mathbf{j}$ are the current and salt flux densities respectively. These flux densities can be written as (see eqns. (2.1a) and (2.1b) in the manuscript): $\mathbf{i} = Pe\mathbf{v}\rho - \boldsymbol{\nabla}\rho - c\boldsymbol{\nabla}(\phi + \phi_{ext})$ and $\mathbf{j} = Pe\mathbf{v}c - \boldsymbol{\nabla}c - \rho\boldsymbol{\nabla}(\phi + \phi_{ext})$, wherein the following char. scale has been chosen for the flux: $i_c \sim j_c \sim Dc_0'/a$. In the inner layer, the flux components have to be rescaled as follows [1, 2]: $i_r \to \delta^{-1}\tilde{I}_r,\ i_\theta \to \tilde{I}_\theta$ and $i_\varphi \to \tilde{I}_\varphi$, wherein $\tilde{I}_k$ $(k = r,\ \theta,\ \varphi) \sim \mathcal{O}(1)$. Similar rescaling also applies to the salt flux. After rescaling, the salt and charge conservation equations in the inner layer may be expressed as:

$$\frac{\partial}{\partial R}\left\{(1+\delta R)^2 \tilde{\Theta}_r\right\} + \delta^2 (1+\delta R)\left[\frac{\partial}{\partial \mu}\left(\sqrt{1-\mu^2}\tilde{\Theta}_\theta\right) + \frac{1}{\sqrt{1-\mu^2}}\frac{\partial \tilde{\Theta}_\varphi}{\partial \varphi}\right] = 0, \tag{S3}$$

where, Θ is the flux density of a generic quantity and may represent both current ($\tilde{\Theta} = \tilde{I}$) or the salt flux ($\tilde{\Theta} = \tilde{J}$). The matching condition for the fluxes then take the following form [1]:

$$\lim_{R\to\infty}[\delta^{-1}\tilde{I}_r,\ \delta^{-1}\tilde{J}_r] = \lim_{r\to 1}[i_r,\ j_r] \tag{S4}$$

We may now use eqn. (S3) to evaluate the LHS of the above matching conditions [2]. To this end, eqn. (S3) may be integrated in R to write:

$$\lim_{R\to\infty}\tilde{\Theta}_r = -\lim_{R\to\infty}\frac{\delta^2}{(1+\delta R)^2}\int_0^R \left(1+\delta\hat{R}\right)\left[\frac{\partial}{\partial \mu}\left(\sqrt{1-\mu^2}\tilde{\Theta}_\theta\right) + \frac{1}{\sqrt{1-\mu^2}}\frac{\partial \tilde{\Theta}_\varphi}{\partial \varphi}\right] d\hat{R} \tag{S5}$$

Equations (S5) and (S4) may now be combined, along with the expressions for the outer region fluxes given prior to eqn. (S3), to write down explicit matching conditions for the net charge and salt concentrations at the edge of the EDL. It then follows from the expressions for $\mathbf{i}$ and $\mathbf{j}$ mentioned earlier that in the leading order of δ, we may write:

$$\frac{\partial c}{\partial r} = \frac{\partial \phi}{\partial r} = 0, \quad \text{at, } r = 1. \tag{S6}$$

This is the eqn. (3.8) in the manuscript.

S1.3 Derivation of rescaled constitutive relations inside the EDL - Eqns. (3.5) of the manuscript

To better illustrate the nature of the constitutive equations presented in (3.5) of the manuscript, we consider two representative stress components and establish their rescaling inside the EDL.

The first example is for the $\theta\theta$ component of the stress, which satisfies the following equation [3] (note that the "dashed" variables denote dimensional quantities with units):

$$\tau'_{\theta\theta} + \lambda'_1 \mathcal{T}'_{\theta\theta} = 2\eta \left[D'_{\theta\theta} + \lambda'_2 \mathcal{S}'_{\theta\theta} \right] \tag{S7a}$$

$$\text{where, } \mathcal{T}'_{\theta\theta} = [\overset{\nabla}{\boldsymbol{\tau}}]'_{\theta\theta} = u'_r \frac{\partial \tau'_{\theta\theta}}{\partial r'} - \frac{u'_\theta \sqrt{1-\mu^2}}{r'} \frac{\partial \tau'_{\theta\theta}}{\partial \mu} + \frac{u'_\varphi}{r'\sqrt{1-\mu^2}} \frac{\partial \tau'_{\theta\theta}}{\partial \varphi} - 2 \Bigg\{ \tau'_{r\theta} \left(\frac{\partial u'_\theta}{\partial r'} - \frac{u'_\theta}{r'} \right)$$

$$+ \frac{\tau'_{\theta\theta}}{r'} \left(u'_r - \sqrt{1-\mu^2} \frac{\partial u'_\theta}{\partial \mu} \right) - \frac{\tau'_{\theta\varphi}}{r'\sqrt{1-\mu^2}} \frac{\partial u'_\theta}{\partial \varphi} \Bigg\} \tag{S7b}$$

Notice that $\mathcal{T}'_{\theta\theta}$ is the $\theta\theta$ component of the convected derivative of the stress and $\mathcal{S}'_{\theta\theta}$ also has analogous expression as given in (S7b), with τ'_{ij} replaced by D'_{ij}.

Now, let us first establish various relevant scales as follows.

$$\underline{\text{1. Outer Region:}}$$

$$\text{Velocity: } u_c \sim \frac{\epsilon k^2 T^2}{e^2 \eta a}; \quad \text{Length: } a; \quad \text{Stresses: } \tau_c \sim \frac{\eta u_c}{a} \tag{S8a}$$

$$\underline{\text{2. Inner Region:}}$$

$$\text{Velocity: } u'_\theta \text{ and } u'_\varphi \sim u_c; \quad u'_r \sim \frac{\lambda_D}{a} u_c \sim \delta u_c; \quad \text{Length: } \lambda_D$$

$$\tau'_{rr} \sim \tau_c; \quad \text{Shear Stresses: } \tau'_{r\theta}, \text{ and } \tau'_{r\varphi} \sim \tau^{EDL}_{s,c} = \frac{\eta u_c}{\lambda_D} = \delta^{-1} \tau_c \tag{S8b}$$

$$\text{Other extensional stresses: } \tau'_{\theta\theta}, \tau'_{\varphi\varphi} \text{ and } \tau'_{\theta\varphi} \sim \tau^{EDL}_{ex,c}$$

Recall that in the above equations, λ_D is the Debye length (characteristics thickness of the EDL) and $\lambda_D/a = \delta$. In the inner layer, we have assumed that the shear stresses ($\tau'_{r\theta}$, $\tau'_{r\varphi}$) and the extensional stresses ($\tau'_{\theta\theta}$, $\tau'_{\varphi\varphi}$ and $\tau'_{\theta\varphi}$) scale differently. First, notice that $\tau'_{rr} \sim \tau_c$ - this may be attributable to the fact that the Oldroyd-B fluids have zero second normal stress coefficient [3]. Further, because this model does not predict shear thinning, it is expected that the shear stresses inside the EDL will scale as: $\tau'_{r\theta} \sim \frac{\eta u_c}{\lambda_D} = \tau^{EDL}_{s,c}$, which may be rewritten as: $\delta^{-1}\tau_c$. This is exactly same as a Newtonian fluid and also exactly same as what has been represented in Table 1 of the manuscript. However, so far, we have not assumed anything about the characteristic magnitude of the extensional stresses, $\tau^{EDL}_{ex,c}$. Once $\tau^{EDL}_{s,c}$ (scale for shear stress) is fixed, this scale may be worked out from (S7a). Notice that so far, for estimating the orders of the stress components, we have also not encountered Deborah number anywhere.

Let us now examine the orders of magnitudes of different terms appearing in $\mathcal{T}'_{\theta\theta}$ in (S7b). All the terms containing extensional stresses, such as $u'_r \frac{\partial \tau'_{\theta\theta}}{\partial r'}$, $\frac{u'_\theta \sqrt{1-\mu^2}}{r'} \frac{\partial \tau'_{\theta\theta}}{\partial \mu}$, $\frac{\tau'_{\theta\varphi}}{r'\sqrt{1-\mu^2}} \frac{\partial u'_\theta}{\partial \varphi}$, etc., scale as: $\left(\frac{u_c}{a}\right) \tau^{EDL}_{ex,c}$. On the other hand, the only term containing the shear stress, i.e., $\tau'_{r\theta} \left(\frac{\partial u'_\theta}{\partial r'} - \frac{u'_\theta}{r'} \right)$ scales as: $\frac{u_c}{\lambda_D} \tau^{EDL}_{s,c} = \delta^{-1} \left(\frac{u_c}{a}\right) \tau^{EDL}_{s,c}$. Therefore, the left hand side of eqn. (S7a) contains terms that obey the following scaling behavior: (i) the first term, $\tau'_{\theta\theta} \sim \tau^{EDL}_{ex,c}$; (ii) terms in $\lambda'_1 \mathcal{T}'_{\theta\theta}$ that contain extensional stresses: $\frac{\lambda_0 u_c}{a} \tau^{EDL}_{ex,c}$ and (iii) finally the term containing shear stress, $\delta^{-1} \frac{\lambda_0 u_c}{a} \tau^{EDL}_{s,c}$. Note that we have assumed $\lambda'_1 \sim \lambda'_2 \sim \lambda_0$. Now, if one defines $De = \frac{\lambda_0 u_c}{a}$ as

the nominal Deborah number and sets $De \sim \mathcal{O}(1)$, it follows that the left hand side of eqn. (S7a) contains terms with two distinct scales: (i) $\tau_{ex,c}^{EDL}$ and (ii) $\delta^{-1}\tau_{s,c}^{EDL}$. Since this equation must retain $\tau_{\theta\theta}$, it follows that $\tau_{ex,c}^{EDL} = \delta^{-1}\tau_{s,c}^{EDL} = \delta^{-2}\tau_c$. This is exactly the same scaling that represents the extensional stresses in the manuscript - see Table 1. An explanation for why this scaling is observed has been presented in details after eqns. (3.4) of the manuscript.

Now, we may define non-dimensional stresses inside the EDL as follows: $\tilde{\tau}_{\theta\theta} = \frac{\tau'_{\theta\theta}}{\delta^{-2}\tau_c}$, $\tilde{\tau}_{\theta\varphi} = \frac{\tau'_{\theta\varphi}}{\delta^{-2}\tau_c}$, $\tilde{\tau}_{r\theta} = \frac{\tau'_{r\theta}}{\delta^{-1}\tau_c}$ etc., such that all these dimensionless stresses are $\mathcal{O}(1)$. We further enforce, $\frac{\partial}{\partial r'} = \frac{1}{\lambda_D}\frac{\partial}{\partial R} = \delta^{-1}a^{-1}\frac{\partial}{\partial R}$ and normalize the velocity components with their respective characteristic scales inside the EDL, as mentioned above in eqns. (S8a) and (S8b). Analogously, the right hand side of eqn. (S7a) may also be scaled in the same way - we do not mention that to avoid repetition. It then directly follows that the leading order (in δ) non-dimensional version of the $\theta\theta$ component given in (S7a) inside the EDL takes the following form:

$$\tilde{\tau}_{\theta\theta} + \lambda_1 De\tilde{\mathcal{T}}_{\theta\theta} = 2\lambda_2 De\tilde{\mathcal{S}}_{\theta\theta} \tag{S9}$$

where, it may be verified that the expressions for $\tilde{\mathcal{T}}_{\theta\theta}$ and $\tilde{\mathcal{S}}_{\theta\theta}$ are exactly the same as given in (3.5b), (A1d) and (A2d) in the manuscript.

At this point, it may be noted that if one defines $De_{EDL} = \delta^{-1}De = \lambda_0 u_c/\lambda_D$ as the characateristic Deborah number inside the EDL, the terms containing the shear stresses in $\lambda_1'\mathcal{T}'_{\theta\theta}$ would then scale as: $De_{EDL}\tau_{s,c}^{EDL} = De_{EDL}\delta^{-1}\tau_c$. But since $De_{EDL} \sim \mathcal{O}(\delta^{-1})$, it follows that this same scale may also be represented as: $\delta^{-1}\tau_{s,c}^{EDL} = \delta^{-2}\tau_c$, which is identical to how we have scaled the extensional stresses (except τ'_{rr}) inside the EDL. The argument presented here indicates how defining a characteristic Deborah number inside the EDL as $De_{EDL} = \lambda_0 u_c/\lambda_D$ is exactly equivalent to re-scaling the shear stresses as $\delta^{-1}\tau_c$ and the extensional stresses as $\delta^{-2}\tau_c$ inside the EDL.

The contextual appropriateness of the Oldroyd-B model and the scaling mentioned above is that its consistency may be checked, by non-dimensionalizing the equation for $\tau'_{r\theta}$ inside the EDL with the same characteristic scales as mentioned above, and then observe whether the same fits in. This aspect is further elucidated below.

The dimensional version for the $r\theta$ component of stress reads:

$$\tau'_{r\theta} + \lambda_1'\mathcal{T}'_{r\theta} = 2\eta\left[D'_{r\theta} + \lambda_2'\mathcal{S}'_{r\theta}\right] \tag{S10a}$$

$$\begin{aligned}\text{where, } \mathcal{T}'_{r\theta} = [\overset{\nabla}{\boldsymbol{\tau}}]'_{r\theta} = {} & u'_r\frac{\partial\tau'_{r\theta}}{\partial r'} - \frac{u'_\theta\sqrt{1-\mu^2}}{r'}\frac{\partial\tau'_{r\theta}}{\partial\mu} + \frac{u'_\varphi}{r'\sqrt{1-\mu^2}}\frac{\partial\tau'_{r\theta}}{\partial\varphi} - \tau'_{rr}\left(\frac{\partial u'_\theta}{\partial r'} - \frac{u'_\theta}{r'}\right) \\ & - \tau'_{r\theta}\left(\frac{\partial u'_r}{\partial r'} + \frac{u'_r}{r'} - \frac{\sqrt{1-\mu^2}}{r'}\frac{\partial u'_\theta}{\partial\mu}\right) - \frac{\tau'_{r\varphi}}{r'\sqrt{1-\mu^2}}\frac{\partial u'_\theta}{\partial\varphi} \\ & + \frac{\tau'_{\theta\theta}\sqrt{1-\mu^2}}{r'}\frac{\partial u'_r}{\partial\mu} - \frac{\tau'_{\theta\varphi}}{r'\sqrt{1-\mu^2}}\frac{\partial u'_r}{\partial\varphi}\end{aligned} \tag{S10b}$$

Let us again examine the orders of magnitudes of different terms appearing in (S10a). In view of the scales we have already discussed in relation to the $\theta\theta$ component of the stress in (S7), it is straightforward to show that the dominant scale in all the terms in $\mathcal{T}'_{r\theta}$ appearing in (S10b) is simply, $\frac{u_c}{a}\tau_{s,c}^{EDL} = \left(\frac{u_c}{a}\right)\delta^{-1}\tau_c$. We would like to clarify that to arrive at this conclusion, one has to take into account that $\tau_{ex,c}^{EDL} \sim \delta^{-1}\tau_{s,c}^{EDL}$ inside the EDL. Therefore, overall the term $\lambda_1'\mathcal{T}'_{r\theta}$ scales as $\left(\frac{\lambda_0 u_c}{a}\right)\tau_{s,c}^{EDL}$. Since we have already enforced $De = \frac{\lambda_0 u_c}{a} \sim \mathcal{O}(1)$, it follows that all the terms on the left hand side scale as: $\tau_{s,c}^{EDL} = \delta^{-1}\tau_c$. The right hand side of eqn. (S10a) may also be scaled analogously inside the EDL and we do not mention that here for the sake of brevity.

Now, if one enforces the non-dimensionalization scheme mentioned before (S9) for all quantities inside the EDL, it may be easily verified that in the leading order of δ, we get the following equation for $\tilde{\tau}_{r\theta}$:

$$\tilde{\tau}_{r\theta} + \lambda_1 De \tilde{\mathcal{T}}_{r\theta} = 2\left[\tilde{D}_{r\theta} + \lambda_2 De \tilde{\mathcal{S}}_{r\theta}\right] \tag{S11}$$

In the above, $\tilde{\mathcal{T}}_{r\theta}$, $\tilde{D}_{r\theta}$ and $\tilde{\mathcal{S}}_{r\theta}$ are identical to those in eqns. (3.5a), (A1b), (A2b) and (A4) in the manuscript and nominally they are all $\mathcal{O}(1)$. Likewise, the rescaled forms of the equations given in eqn. (3.5) and Appendix-A of the manuscript for other stress components, may also be verified.

Notice that in deriving (S9) and (S11) by enforcing the scaling inside the EDL, we have never used the fact that the surface charge is weak. Therefore, these scalings are valid as long as the characteristic velocity scales as u_c. Now, for a weakly charged particle, $\bar{\zeta}_0 \ll 1$ (see the manuscript for definition), and therefore the flow will be weak in nature. Thus, the non-dimensional velocity (u_θ, u_φ etc.) in both the regions will at the most scale as $\mathcal{O}(\bar{\zeta}_0)$, which means that the appropriately normalized stresses would scale at the most as $\mathcal{O}(\bar{\zeta}_0)$ everywhere. Therefore, it naturally follows that the non-linear terms represented by $\tilde{\mathcal{T}}_{r\theta}$, $\tilde{\mathcal{T}}_{\theta\theta}$, etc. would scale at the most as $\mathcal{O}(\bar{\zeta}_0^2)$. Consequently, if we expand all variables in an asymptotic series of $\bar{\zeta}_0$, in the leading order of $\bar{\zeta}_0$, only linear Newtonian-like contributions will be present and the non-linear components of the polymeric stresses given by $\tilde{\mathcal{T}}_{r\theta}$ etc., would start to contribute from $\mathcal{O}(\bar{\zeta}_0^2)$ onwards. Therefore, the flow is effectively Newtonian in the leading order of $\bar{\zeta}_0$ and viscoelastic effects play a subdominant role to an extent to influence higher order effects only. In other words, the overall transport is weakly viscoelastic. Considering that the asymptotic expansion in $\bar{\zeta}_0$ may also be treated as an expansion in $De_{eff} = De\bar{\zeta}_0 \sim \mathcal{O}(\bar{\zeta}_0)$, it is imperative that the flow is effectively weakly viscoelastic, despite nominally $De \sim \mathcal{O}(1)$.

S1.4 Velocity field in the Inner layer and the Modified Smoluchowski Slip

We first note that in presence of particle rotation, the "*Modified Smoluchowski Slip*" will be defined as: $\mathbf{v}_S = \lim_{R\to\infty}[U\hat{\mathbf{e}}_\theta + W\hat{\mathbf{e}}_\phi] - \boldsymbol{\Omega}\times\hat{\mathbf{e}}_r$. Recall that in the inner layer, the velocity field has the expansion: $\mathbf{V} = \bar{\zeta}_0\mathbf{V}_1 + \bar{\zeta}_0^2\mathbf{V}_2 + \bar{\zeta}_0^3\mathbf{V}_3 + ...$, where $\mathbf{V} = U\hat{\mathbf{e}}_\theta + W\hat{\mathbf{e}}_\varphi + V\hat{\mathbf{e}}_r$. Further recall that (see §3.4 in the main manuscript) both U and W remain bounded inside the EDL and on the particle surface, $\mathbf{V}$ satisfies the following b.c.: $\mathbf{V}(R=0) = \boldsymbol{\Omega}\times\hat{\mathbf{e}}_r = \Gamma\hat{\mathbf{e}}_\theta + \chi\hat{\mathbf{e}}_\varphi$. Recall that, $\Gamma = (\boldsymbol{\Omega}\times\hat{\mathbf{e}}_r)\cdot\hat{\mathbf{e}}_\theta = \Omega_y\cos(\varphi) - \Omega_x\sin(\varphi)$ and $\chi = (\boldsymbol{\Omega}\times\hat{\mathbf{e}}_r)\cdot\hat{\mathbf{e}}_\varphi = -\left(\Omega_x\cos(\varphi) + \Omega_y\sin(\varphi)\right)\cos(\theta) + \boldsymbol{\Omega}_z\sin\theta$. The $\mathcal{O}(\bar{\zeta}_0)$ and $\mathcal{O}(\bar{\zeta}_0^2)$ velocity fields in the EDL and the resulting modified Smoluchowski slip, accounting for particle rotation have already been mentioned in §3.4 of the main manuscript - see eqns. (3.14) and (3.18) therein. However, in eqn. (3.20) of the manuscript, the corrections to the Smoluchowski slip at $\mathcal{O}(\bar{\zeta}_0^3)$ was reported only for non-rotating particles. Here the complete results for the $\mathcal{O}(\bar{\zeta}_0^3)$ modified Smoluchowski slip in the presence of particle rotation has been discussed.

At $\mathcal{O}(\bar{\zeta}_0^3)$, the velocity field satisfies the equations (see eqns. (3.19) in the manuscript):

$$\frac{\partial^2 U_3}{\partial R^2} = 2(\lambda_1-\lambda_2)De\tilde{\boldsymbol{\nabla}}\cdot\left[\left(\tilde{\boldsymbol{\mathcal{S}}} - \lambda_1 De\Im\right)\cdot\hat{\mathbf{e}}_\theta\right] - \frac{3}{2}\beta\sqrt{1-\mu^2}\frac{\partial^2\Phi_3}{\partial R^3} \tag{S12a}$$

$$\frac{\partial^2 W_3}{\partial R^2} = 2(\lambda_1-\lambda_2)De\tilde{\boldsymbol{\nabla}}_*\cdot\left[\left(\tilde{\boldsymbol{\mathcal{S}}} - \lambda_1 De\Im\right)\cdot\hat{\mathbf{e}}_\varphi\right] \tag{S12b}$$

where, $\tilde{\boldsymbol{\nabla}} = \hat{\mathbf{e}}_r\frac{\partial}{\partial R} - \hat{\mathbf{e}}_\theta\frac{\partial}{\partial\mu}\sqrt{1-\mu^2} + \hat{\mathbf{e}}_\varphi\frac{\partial}{\partial\varphi}$ and $\tilde{\boldsymbol{\nabla}}_* = \hat{\mathbf{e}}_r\frac{\partial}{\partial R} - \hat{\mathbf{e}}_\theta\frac{\partial}{\partial\mu}\sqrt{1-\mu^2} + \hat{\mathbf{e}}_\varphi\frac{\mu}{\sqrt{1-\mu^2}}$. The various components of $\tilde{\boldsymbol{\mathcal{S}}}$ have been mentioned in Appendix-A of the main manuscript. The

required components of $\mathfrak{F}$ may be expressed as follows:

$$\mathfrak{F}_{r\theta} = \frac{D^{(1)}\tilde{\mathcal{S}}^{(2)}_{r\theta}}{Dt} - \tilde{\mathcal{S}}^{(2)}_{rr}\frac{\partial U_1}{\partial R} - \tilde{\mathcal{S}}^{(2)}_{r\theta}\left(\frac{\partial V_1}{\partial R} - \sqrt{1-\mu^2}\frac{\partial U_1}{\partial \mu}\right) - \frac{\tilde{\mathcal{S}}^{(2)}_{r\varphi}}{\sqrt{1-\mu^2}}\frac{\partial U_1}{\partial \varphi} + \sqrt{1-\mu^2}\tilde{\mathcal{S}}^{(2)}_{\theta\theta}\frac{\partial V_1}{\partial \mu} \tag{S13a}$$

$$\mathfrak{F}_{\theta\theta} = \frac{D^{(1)}\tilde{\mathcal{S}}^{(2)}_{\theta\theta}}{Dt} - 2\tilde{\mathcal{S}}^{(2)}_{r\theta}\frac{\partial U_1}{\partial R} + 2\tilde{\mathcal{S}}^{(2)}_{\theta\theta}\sqrt{1-\mu^2}\frac{\partial U_1}{\partial \mu} \tag{S13b}$$

$$\mathfrak{F}_{r\varphi} = \frac{D^{(1)}\tilde{\mathcal{S}}^{(2)}_{r\varphi}}{Dt} + \tilde{\mathcal{S}}^{(2)}_{r\theta}\left(\sqrt{1-\mu^2}\frac{\partial W_1}{\partial \varphi} + \frac{\mu W_1}{\sqrt{1-\mu^2}}\right) - \tilde{\mathcal{S}}^{(2)}_{r\varphi}\left(\frac{1}{\sqrt{1-\mu^2}}\frac{\partial W_1}{\partial \varphi} \frac{\partial V_1}{\partial R} + \frac{\mu U_1}{\sqrt{1-\mu^2}}\right) \tag{S13c}$$

$$\mathfrak{F}_{\theta\varphi} = -\tilde{\mathcal{S}}^{(2)}_{r\varphi}\frac{\partial U_1}{\partial R} - \tilde{\mathcal{S}}^{(2)}_{\theta\theta}\left(\frac{\mu W_1}{\sqrt{1-\mu^2}} - \sqrt{1-\mu^2}\frac{\partial W_1}{\partial \mu}\right) \tag{S13d}$$

$$\text{where, } \frac{D^{(k)}\xi}{Dt} = V_k\frac{\partial \xi}{\partial R} - \sqrt{1-\mu^2}U_k\frac{\partial \xi}{\partial \mu} + \frac{W_k}{\sqrt{1-\mu^2}}\frac{\partial \xi}{\partial \varphi}$$

Eqns. (S12) may be solved subject to appropriate boundary condtions (see at the beginning of §S1.4), from which the $\mathcal{O}(\bar{\zeta}_0^3)$ slip velocity might be deduced. The final result for the slip velocity takes the following form:

$$\mathbf{v}_S^{(3)} = \lim_{R\to\infty}[U_3\hat{\mathbf{e}}_\theta + W_3\hat{\mathbf{e}}_\phi] - \mathbf{\Omega}_3\times\hat{\mathbf{e}}_r = v^{(3)}_{S,\theta}\hat{\mathbf{e}}_\theta + v^{(3)}_{S,\varphi}\hat{\mathbf{e}}_\varphi \tag{S14a}$$

$$v^{(3)}_{S,\theta} = \mathbf{v}_S^{(3)}\cdot\hat{\mathbf{e}}_\theta = De^2\mathbb{U}_2 + De\mathbb{U}_1 + \mathbb{U}_0 \tag{S14b}$$

$$v^{(3)}_{S,\varphi} = \mathbf{v}_S^{(3)}\cdot\hat{\mathbf{e}}_\varphi = De^2\mathbb{W}_1 + De\mathbb{W}_2$$

$$\text{where, } \mathbb{U}_0 = -\frac{1}{16}\bar{\zeta}^3\beta\sqrt{1-\mu^2} \tag{S14c}$$

$$\mathbb{U}_1 = \omega_1\mathcal{H}_1(\mu,\varphi) + \mathcal{H}_0(\mu,\varphi) \tag{S14d}$$

$$\mathbb{U}_2 = \omega_1^3 G_3(\mu,\varphi) + \omega_1^2 G_2(\mu,\varphi) + \omega_1 G_1(\mu,\varphi) + G_0(\mu,\varphi) \tag{S14e}$$

$$\text{with, } \mathcal{H}_1 = \frac{3\beta(\lambda_2-\lambda_1)}{1-\mu^2}\left(3\mu\Gamma_2 - 4\chi_{2,\varphi}\right) \tag{S14f}$$

$$\mathcal{H}_0 = \frac{3\beta(\lambda_2-\lambda_1)}{1-\mu^2}\left\{\chi_2\omega_{1,\varphi} - \Gamma_2\omega_{1,\mu}(1-\mu^2)\right\} \tag{S14g}$$

$$\mathbb{W}_2 = -\frac{3\beta(\lambda_2-\lambda_1)}{1-\mu^2}\left\{\chi_{2,\varphi}(\mu^2-1) - \mu\chi_2\right\}\omega_1 \tag{S14h}$$

$$\mathbb{W}_1 = \mathcal{K}_1\omega_1^2 + \mathcal{K}_2\omega_1 + \mathcal{K}_3\omega_{1,\mu} + \mathcal{K}_4\omega_{1,\varphi} \tag{S14i}$$

Expressions for G_j ($j = 1-3$) and $\mathcal{K}_i$ ($i = 1-4$) have been given in the next subsection (see §S1.5). We reiterate that eqn. (3.20) in the main manuscript may be recovered by enforcing $\Gamma_2 = \chi_2 = \Gamma_1 = \chi_1 = 0$ in the above expressions. Notice that the rotation only influences the slip velocity from $\mathcal{O}(\bar{\zeta}_0^2)$ onwards, as is obviously true at $\mathcal{O}(\bar{\zeta}_0^3)$, evident from (S14) here and eqns. (3.18) of the main manuscript. This is a unique result for viscoelastic medium and to the best of our knowledge, ours is the first study to bring this effect to light. More discussions on this topic has been included in §3.5 and §5 of the main manuscript. Further observe that at $\mathcal{O}(\bar{\zeta}_0^2)$ and also at subsequent higher orders, W becomes a function of R, whereas in Newtonian

fluids, W (within the EDL) will simply be the local velocity at the particle surface. As a result, particle's angular velocity makes the flow within the EDL fully 3-dimensional. The same is also expected of the outer layer because of inherent anisotropy in the Smoluchowski slip boundary condition, applicable to the flow in that region. Such physical paradigms may result in anisotropic drag on the particle [4], which might lead to a mismatch between the velocity of the particle ($\mathcal{U}\hat{\mathbf{e}}_u$) and the direction of the imposed electric field.

S1.5 Expressions for the constants G_j's and $\mathcal{K}_j$'s in Eqns. (S14)

The functions G_j's ($j = 1 - 3$) are as follows:

$$G_3 = -\frac{3\beta^3(\lambda_1-\lambda_2)^2}{2(1-\mu^2)^{5/2}}\left(37\mu^2+29\right) \tag{S15a}$$

$$G_2 = \gamma_1\omega_{1,\mu}+\gamma_2\omega_{1,\mu\mu}+\gamma_3\Gamma_1+\gamma_4\chi_{1,\varphi}+\gamma_5\chi_{1,\mu\varphi}+\gamma_6\chi_{1,\varphi\varphi}+\gamma_7\omega_2+\gamma_8\omega_{2,\mu}+\gamma_9\omega_{3,\varphi} \tag{S15b}$$

$$\text{where, } \gamma_1 = \frac{81\beta^3\mu(\lambda_2-\lambda_1)}{2(1-\mu^2)^{3/2}}\left(4\lambda_1-5\lambda_2\right);\ \gamma_2 = \frac{27\beta^3(\lambda_2-\lambda_1)}{4(1-\mu^2)^{1/2}}\left(21\lambda_1-34\lambda_2\right) \tag{S15c}$$

$$\gamma_3 = \frac{9\beta^2(\lambda_2-\lambda_1)}{2(1-\mu^2)^2}\left[\lambda_2\left(4\mu^2+7\right)-5\lambda_1\left(\mu^2+3\right)\right] \tag{S15d}$$

$$\gamma_4 = -\frac{27\beta^2\mu(\lambda_2-\lambda_1)}{4(1-\mu^2)^2};\quad \gamma_5 = -(2/3)\gamma_4;\quad \gamma_6 = (1/3)\gamma_4 \tag{S15e}$$

$$\gamma_7 = \frac{9\beta^2\mu(\lambda_2-\lambda_1)}{2(1-\mu^2)^{3/2}}\left(\lambda_1-4\lambda_2\right);\quad \gamma_8 = -\frac{27\beta^2(\lambda_1-\lambda_2)^2}{\sqrt{1-\mu^2}};\quad \gamma_9 = -\frac{45\beta^2(\lambda_1-\lambda_2)^2}{2(1-\mu^2)^{3/2}} \tag{S15f}$$

$$G_1 = L_1\omega_{1,\mu}^2+L_2\omega_{1,\mu}+L_3\omega_{1,\varphi}+L_4\omega_{1,\mu\varphi}+L_5\omega_{1,\mu\mu}+L_6\Gamma_1+L_7\Gamma_1^2+L_8\Gamma_{1,\varphi}+L_9\omega_2^2+L_{10}\chi_1 \tag{S15g}$$

$$\text{where, } L_1 = \frac{27\beta^3(\lambda_2-\lambda_1)}{\sqrt{1-\mu^2}}\left(11\lambda_1-18\lambda_2\right) \tag{S15h}$$

$$L_2 = -\frac{9\beta^2(\lambda_2-\lambda_1)\mu}{2(1-\mu^2)}\left(5\lambda_1-16\lambda_2\right)\Gamma_1+\frac{9\beta^2(\lambda_2-\lambda_1)}{\sqrt{1-\mu^2}}\left(5\lambda_1-8\lambda_2\right)\omega_2 \tag{S15i}$$

$$L_3 = \frac{45\beta^2(\lambda_2-\lambda_1)\mu}{2(1-\mu^2)^2}\left(\lambda_1-2\lambda_2\right)\chi_1+\frac{9\beta^2(\lambda_2-\lambda_1)\mu}{(1-\mu^2)}\left(2\lambda_1-3\lambda_2\right)\chi_{1,\mu}-\frac{27\beta^2(\lambda_2-\lambda_1)^2}{2(1-\mu^2)^{3/2}}\omega_3 \tag{S15j}$$

$$L_4 = \frac{9(\lambda_2-\lambda_1)\beta^2}{1-\mu^2}\left(\lambda_1-6\lambda_2\right)\chi_1;\quad L_5 = -(1-\mu^2)L_4(\Gamma_1/\chi_1) \tag{S15k}$$

$$L_6 = \frac{6\beta\lambda_2(\lambda_2-\lambda_1)\mu}{1-\mu^2}\omega_2+3\lambda_2\beta\left(\lambda_2-\lambda_1\right)\omega_{2,\mu};\quad L_7 = -\frac{3\beta\lambda_2(\lambda_2-\lambda_1)}{(1-\mu^2)^{3/2}}(1+\mu^2) \tag{S15l}$$

$$L_8 = -\frac{3\beta(\lambda_2-\lambda_1)^2}{1-\mu^2}\omega_3+\frac{3\beta\mu(\lambda_2^2-\lambda_1^2)}{(1-\mu^2)^{3/2}}\chi_1+\frac{3\beta\lambda_1(\lambda_2-\lambda_1)}{\sqrt{1-\mu^2}}\chi_{1,\varphi} \tag{S15m}$$

$$L_9 = \frac{3\beta\lambda_2(\lambda_1-\lambda_2)}{\sqrt{1-\mu^2}};\quad L_{10} = \frac{3\beta\lambda_2(\lambda_1-\lambda_2)}{1-\mu^2}\omega_{2,\varphi} \tag{S15n}$$

$$G_0 = J_1\omega_{1,\mu}^2+J_2\omega_{1,\mu}+J_3\omega_{1,\varphi}+J_4\omega_{1,\mu\varphi}+J_5\omega_{1,\varphi\varphi}+J_6\omega_{1,\mu\mu} \tag{S15o}$$

$$\text{with, } J_1 = 18(\lambda_1-\lambda_2)\beta^2(\lambda_1-3\lambda_2)\Gamma_1 \tag{S15p}$$

$$J_2 = \frac{18(\lambda_1-\lambda_2)\beta^2(\lambda_1-3\lambda_2)}{1-\mu^2}\chi_1\omega_{1,\varphi}+\frac{3\mu\lambda_2(\lambda_1-\lambda_2)}{\sqrt{1-\mu^2}}\Gamma_1^2+6\beta\lambda_2(\lambda_2-\lambda_1)\Gamma_1\omega_2$$

$$+\frac{3\beta\lambda_2(\lambda_2-\lambda_1)}{\sqrt{1-\mu^2}}\chi_1\Gamma_{1,\varphi} \tag{S15q}$$

$$J_3=\frac{3\beta\lambda_2(\lambda_2-\lambda_1)}{(1-\mu^2)^{3/2}}\left\{(1-\mu^2)\chi_{1,\mu}+3\mu\chi_1\right\}\Gamma_1+\frac{6\beta\lambda_2(\lambda_1-\lambda_2)}{1-\mu^2}\chi_1\omega_2$$
$$\frac{3\beta\lambda_2(\lambda_1-\lambda_2)}{(1-\mu^2)^{3/2}}\chi_1\chi_{1,\varphi} \tag{S15r}$$

$$J_4=\frac{6\beta\lambda_2(\lambda_2-\lambda_1)}{(1-\mu^2)^{1/2}}\chi_1\Gamma_1;\ J_5=\frac{3\beta\lambda_2(\lambda_1-\lambda_2)}{(1-\mu^2)^{3/2}}\chi_1^2;\ J_6=3\lambda_2(\lambda_1-\lambda_2)\beta\sqrt{1-\mu^2}\Gamma_1 \tag{S15s}$$

The functions $\mathcal{K}_j$'s ($j=1-4$) have the following expressions:

$$\mathcal{K}_1=\mathcal{K}_{11}\omega_3+\mathcal{K}_{12}\omega_{3,\mu}+\mathcal{K}_{13}\omega_{3,\varphi}+\mathcal{K}_{14}\chi_1+\mathcal{K}_{15}\chi_{1,\mu}+\mathcal{K}_{16}\chi_{1,\varphi}+\mathcal{K}_{17}\chi_{1,\varphi\mu}+\mathcal{K}_{18}\chi_{1,\mu\mu} \tag{S16a}$$

$$\mathcal{K}_{11}=\frac{9\beta^2(\lambda_1-\lambda_2)^2\mu}{2(1-\mu^2)^{3/2}};\ \mathcal{K}_{12}=\frac{9\beta^2(\lambda_1-\lambda_2)^2}{(1-\mu^2)^{1/2}};\ \mathcal{K}_{13}=-\frac{1}{2}\mathcal{K}_{12} \tag{S16b}$$

$$\mathcal{K}_{14}=\frac{9\beta^2(\lambda_1-\lambda_2)\left(\mu^2(\lambda_1+\lambda_2)+\frac{5\lambda_1}{2}\right)}{2(1-\mu^2)^2};\ \mathcal{K}_{15}=-\frac{27\lambda_1\beta^2(\lambda_2-\lambda_1)\mu}{4(1-\mu^2)} \tag{S16c}$$

$$\mathcal{K}_{16}=\mathcal{K}_{15}\left(1-2\frac{\lambda_2}{\lambda_1}\right);\ \mathcal{K}_{17}=\frac{27}{4}\lambda_1\beta^2(\lambda_1-\lambda_2);\ \mathcal{K}_{18}=\frac{3}{2}\mathcal{K}_{17} \tag{S16d}$$

$$\mathcal{K}_2=\mathcal{K}_{21}\omega_{1,\mu}+\mathcal{K}_{22}\omega_{1,\varphi}+\mathcal{K}_{23}\omega_3+\mathcal{K}_{24}\omega_{3,\mu}+\mathcal{K}_{25}\omega_{3,\varphi}+\mathcal{K}_{26}\Gamma_1+\mathcal{K}_{27}\omega_2+\mathcal{K}_{28}\chi_{1,\varphi}^2+\mathcal{K}_{29}\chi_{1,\varphi\varphi} \tag{S16e}$$

$$\text{where, }\ \mathcal{K}_{21}=\mathcal{K}_{211}\omega_3+\mathcal{K}_{212}\chi_1+\mathcal{K}_{213}\chi_{1,\mu}+\mathcal{K}_{214}\chi_{1,\varphi};\ \mathcal{K}_{211}=\frac{45\beta^2(\lambda_1-\lambda_2)^2}{2\sqrt{1-\mu^2}} \tag{S16f}$$

$$\mathcal{K}_{212}=-\frac{9\beta^2\lambda_2(\lambda_1-\lambda_2)(2\lambda_1+3\lambda_2)\mu}{1-\mu^2};\ \mathcal{K}_{213}=9\lambda_1\beta^2(\lambda_1-\lambda_2);\ \mathcal{K}_{214}=9\beta^2(\lambda_1-\lambda_2)(\lambda_1+3\lambda_2) \tag{S16g}$$

$$\mathcal{K}_{22}=-\frac{1}{5}\mathcal{K}_{211}\omega_3;\ \ \mathcal{K}_{23}=\mathcal{K}_{231}\Gamma_1+\mathcal{K}_{232}\omega_2+\mathcal{K}_{233}]\chi_{1,\varphi};\ \mathcal{K}_{231}=-\frac{6\beta\mu(\lambda_1-\lambda_2)^2}{1-\mu^2} \tag{S16h}$$

$$\mathcal{K}_{232}=\frac{3\beta(\lambda_1-\lambda_2)^2}{\sqrt{1-\mu^2}};\ \mathcal{K}_{233}=-\frac{\mathcal{K}_{232}}{\sqrt{1-\mu^2}};\ \ \mathcal{K}_{24}=-3\beta(\lambda_1-\lambda_2)^2\Gamma_1 \tag{S16i}$$

$$\mathcal{K}_{25}=-\mathcal{K}_{233}\chi_1;\ \ \mathcal{K}_{26}=\mathcal{K}_{261}\chi_1+\mathcal{K}_{262}\chi_{1,\mu}+\mathcal{K}_{263}\chi_{1,\varphi}+\mathcal{K}_{264}\chi_{1,\mu\varphi} \tag{S16j}$$

$$\mathcal{K}_{261}=\frac{3\beta(\lambda_2-\lambda_1)}{(1-\mu^2)^{3/2}}\left[\lambda_1(1+2\mu^2)+\mu^2\lambda_2\right];\ \mathcal{K}_{262}=\frac{3\beta\mu\lambda_1(\lambda_2-\lambda_1)}{\sqrt{1-\mu^2}} \tag{S16k}$$

$$\mathcal{K}_{263}=\frac{3\beta\mu(\lambda_2^2-\lambda_1^2)}{\sqrt{1-\mu^2}};\ \mathcal{K}_{264}=3\beta\lambda_1(\lambda_2-\lambda_1)\sqrt{1-\mu^2} \tag{S16l}$$

$$\mathcal{K}_{27}=\frac{3\beta(\lambda_1^2-\lambda_2^2)}{1-\mu^2}\left[(1-\mu^2)\chi_{1,\varphi}+\mu\chi_1\right];\ \ \mathcal{K}_{28}=-\frac{3\beta\lambda_1(\lambda_1-\lambda_2)}{\sqrt{1-\mu^2}};\ \ \mathcal{K}_{29}=-\mathcal{K}_{28}\chi_1 \tag{S16m}$$

$$\mathcal{K}_3=3\beta(\lambda_2-\lambda_1)\Gamma_1\left[\frac{\mu(\lambda_1+\lambda_2)}{\sqrt{1-\mu^2}}\chi_1+(\lambda_1+\lambda_2)\sqrt{1-\mu^2}\chi_{1,\varphi}+(\lambda_1-\lambda_2)\omega_3\right] \tag{S16n}$$

$$\mathcal{K}_4=3\beta(\lambda_2-\lambda_1)\left[-\frac{\mu(\lambda_1+\lambda_2)}{(1-\mu^2)^{3/2}}\chi_1^2-\frac{\lambda_1+\lambda_2}{\sqrt{1-\mu^2}}\chi_1\chi_{1,\varphi}+\frac{\lambda_2-\lambda_1}{1-\mu^2}\chi_1\omega_3\right] \tag{S16o}$$

S2 Components of the stream function at $\mathcal{O}(\bar{\zeta}_0^3)$

S2.1 Expression for $\mathcal{N}_1^{(3)}$

Recall that Ψ_3 satisfies the equation: $\mathcal{E}^4\Psi_3 = De^2\beta^3(\lambda_1-\lambda_2)\sum_{n=1}^{6}\mathcal{N}_n^{(3)}(r)Q_n(\mu)$. Further note that $\mathcal{N}_1^{(3)} = \mathcal{P}_1(r)a_0^3 + \mathcal{P}_2(r)a_0a_1^2$. Expressions for $\mathcal{P}_1$ and $\mathcal{P}_2$ are given by the following:

$$\mathcal{P}_1 = \frac{1782(\lambda_2-\lambda_1)}{r^8} - \frac{2580\lambda_1}{r^{10}} + \frac{1224\lambda_1}{r^{13}} \text{ and } \mathcal{P}_2 = \lambda_1\mathcal{P}_{21} + \lambda_2\mathcal{P}_{22} \tag{S17a}$$

$$\text{where, } \mathcal{P}_{21} = \frac{27}{175}\left[\frac{7035}{r^8} + \frac{11375}{r^{10}} + \frac{22896}{r^{11}} - \frac{94500}{r^{12}} - \frac{96700}{r^{13}} + \frac{72000}{r^{15}}\right] \tag{S17b}$$

$$\mathcal{P}_{22} = \frac{27}{175}\left[-\frac{10335}{r^8} + \frac{37625}{r^{10}} - \frac{3456}{r^{11}} - \frac{1600}{r^{13}}\right] \tag{S17c}$$

S2.2 Stream function at $\mathcal{O}(\bar{\zeta}_0^3)$ for a uniformly charged particle

Complete solution for Ψ_3 for the special case of a uniformly charged particle ($a_0 = 1,\ a_1 = 0$) is given by:

$$\Psi_{3,\text{ucp}} = De^2\beta^3(\lambda_1-\lambda_2)\left[\mathbb{M}_1(r)Q_1(\mu) + \mathbb{M}_3(r)Q_3(\mu)\right] \tag{S18a}$$

$$\mathbb{M}_1(r) = \frac{\mathcal{U}_{3,\text{ucp}}r^2}{De^2\beta^3(\lambda_1-\lambda_2)} + b_{11}r + \frac{b_{12}}{r} - \frac{9\left\{\lambda_1(1573r^5+572r^3-68) - 1573\lambda_2r^5\right\}}{5720r^9} \tag{S18b}$$

$$\mathbb{M}_3(r) = \frac{b_{31}}{r} + \frac{b_{32}}{r^3} - \frac{3\left\{\lambda_1(3861r^5+104r^3-16) - 3861\lambda_2r^5\right\}}{520r^9} \tag{S18c}$$

$$b_{11} = -\frac{3\mathcal{U}_{3,\text{ucp}}}{2De^2\beta^3(\lambda_1-\lambda_2)} + \frac{3}{40}(\lambda_1+8\lambda_2) - \frac{12663}{2288}\lambda_1 + \frac{297}{80}\lambda_2 - \frac{\beta}{16De^2\beta^3(\lambda_1-\lambda_2)} \tag{S18d}$$

$$b_{12} = -\frac{3}{40}(\lambda_1+8\lambda_2) + \frac{\mathcal{U}_3}{2De^2\beta^3(\lambda_1-\lambda_2)} + \frac{100701}{11440}\lambda_1 - \frac{99}{16}\lambda_2 + \frac{\beta}{16De^2\beta^3(\lambda_1-\lambda_2)} \tag{S18e}$$

$$b_{31} = \frac{3}{20}(802\lambda_1 - 1369\lambda_2) - \frac{12231}{1040}\lambda_1 + \frac{891}{80}\lambda_2 \tag{S18f}$$

$$b_{32} = \frac{7185}{208}\lambda_1 - \frac{2673}{80}\lambda_2 + \frac{3}{20}(802\lambda_1 - 1369\lambda_2) \tag{S18g}$$

$$\text{and finally, } \mathcal{U}_{3,\text{ucp}} = De^2\beta^3(\lambda_1-\lambda_2)\left(\frac{23}{8}\lambda_2 - \frac{20819}{5720}\lambda_1\right) - \frac{1}{24}\beta \tag{S18h}$$

S3 Numerical simulations for the FENE-P model: the velocity field

In §4.4 of the manuscript, accuracy of the analytical solutions derived using the Oldroyd-B model has been assessed by comparing them with numerical solutions for the FENE-P constitutive model, which is more robust and does not suffer from the many shortcomings of the Oldroyd-B model - also see §3.6 of the manuscript. The detailed governing equations, boundary conditions and the simulation environment along with the mesh have been outlined in §4.4.1 and §4.4.2 in the manuscript. The simulations have been carried out in the commercial software package COMSOL Multiphysics 5.6, using its Polymer flow module. Detailed comparison with analytical solutions have been included in §4.4.3 of the manuscript.

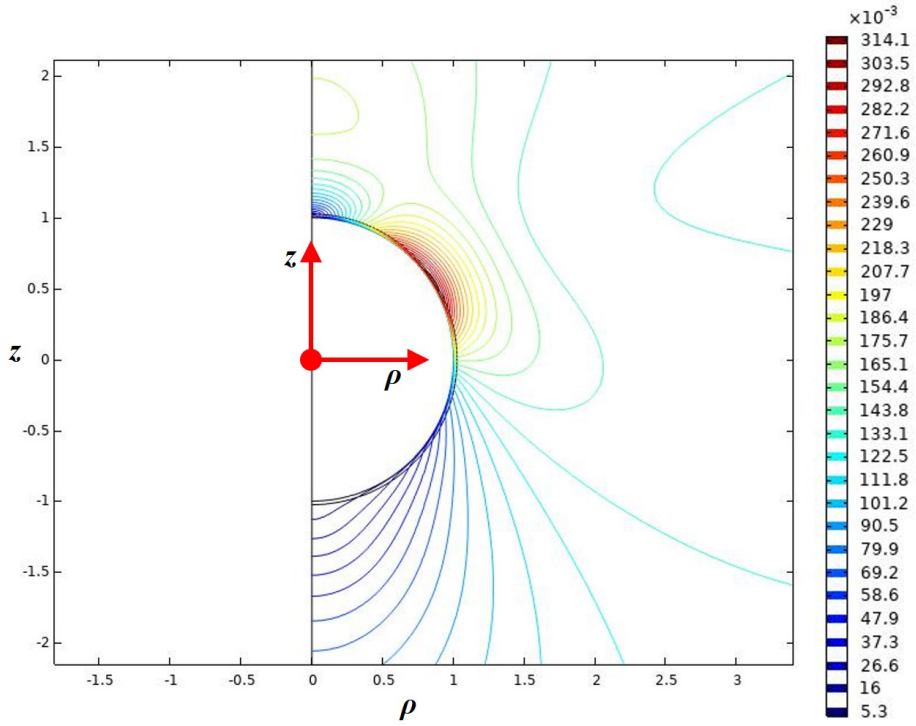

Figure S1: Velocity magnitude contours deduced from the numerical solutions for flow past a spherical axisymmetric particle in a FENE-P fluid. The schematic of the flow domain has been depicted in figure 2 in the manuscript. Here only the region close to the particle has been shown. The particle carries a surface charge of the form: $\zeta(\theta) = \bar{\zeta}_0(a_0 + a_1\mu)$, where $a_0 = a_1 = 1/2$ and $\bar{\zeta}_0 = 0.2$. Other relevant parameters are: $\delta = 0.005$, $\beta = De = 1$, $\mathcal{C} = 1$ and $\ell^2 = 200$.

To complement the discussions in §4.4 of the manuscript, figure S1 here shows a representative contour plot of velocity magnitude, as computed from the numerical solutions for the FENE-P constitutive model. Only the contours close to the particle surface have been shown, while values of other relevant parameters have been mentioned in the caption. Notice the large variations in $|\mathbf{v}|$ around the particle caused by two main factors: (i) the non-uniform charge density on its surface and (ii) presence of a very thin EDL ($\delta = 0.005$), which causes the velocity to vary to rapidly within the Double layer.

S4 Polymeric stresses in the outer layer

To better understand the stress distribution in the bulk, we have now plotted the polymeric stress ($\boldsymbol{\tau}^P$) at $O(\bar{\zeta}_0^2)$, for flow past a non-uniformly charged particle. The charge density is given by: $\bar{\zeta} = a_0 + a_1\mu$ (same as in the manuscript), whereas the polymeric stress (non-dimensional) is governed by the following [3, 5]:

$$\boldsymbol{\tau}^P + De\overset{\nabla}{\boldsymbol{\tau}}^P = 2\left(1 - \frac{\lambda_2}{\lambda_1}\right)\mathbf{D} \tag{S19}$$

where $\mathbf{D}$ is the rate of strain tensor and the charactersitic stress has been chosen as: $\eta u_c/a$, η being the total viscosity of the fluid, i.e., $\eta = \eta^P + \eta^S$. Here is should be noted that $\eta^P/\eta = \mathcal{C}/(1+\mathcal{C}) = 1 - \lambda_2/\lambda_1$, where $\mathcal{C} = \eta^P/\eta^S$ quantifies the polymeric viscosity as compared to the solvent. The polymeric stress $\boldsymbol{\tau}^P$ has the expansion, $\boldsymbol{\tau}^P = \bar{\zeta}_0\boldsymbol{\tau}_1^P + \bar{\zeta}_0^2\boldsymbol{\tau}_2^P + ...$, where

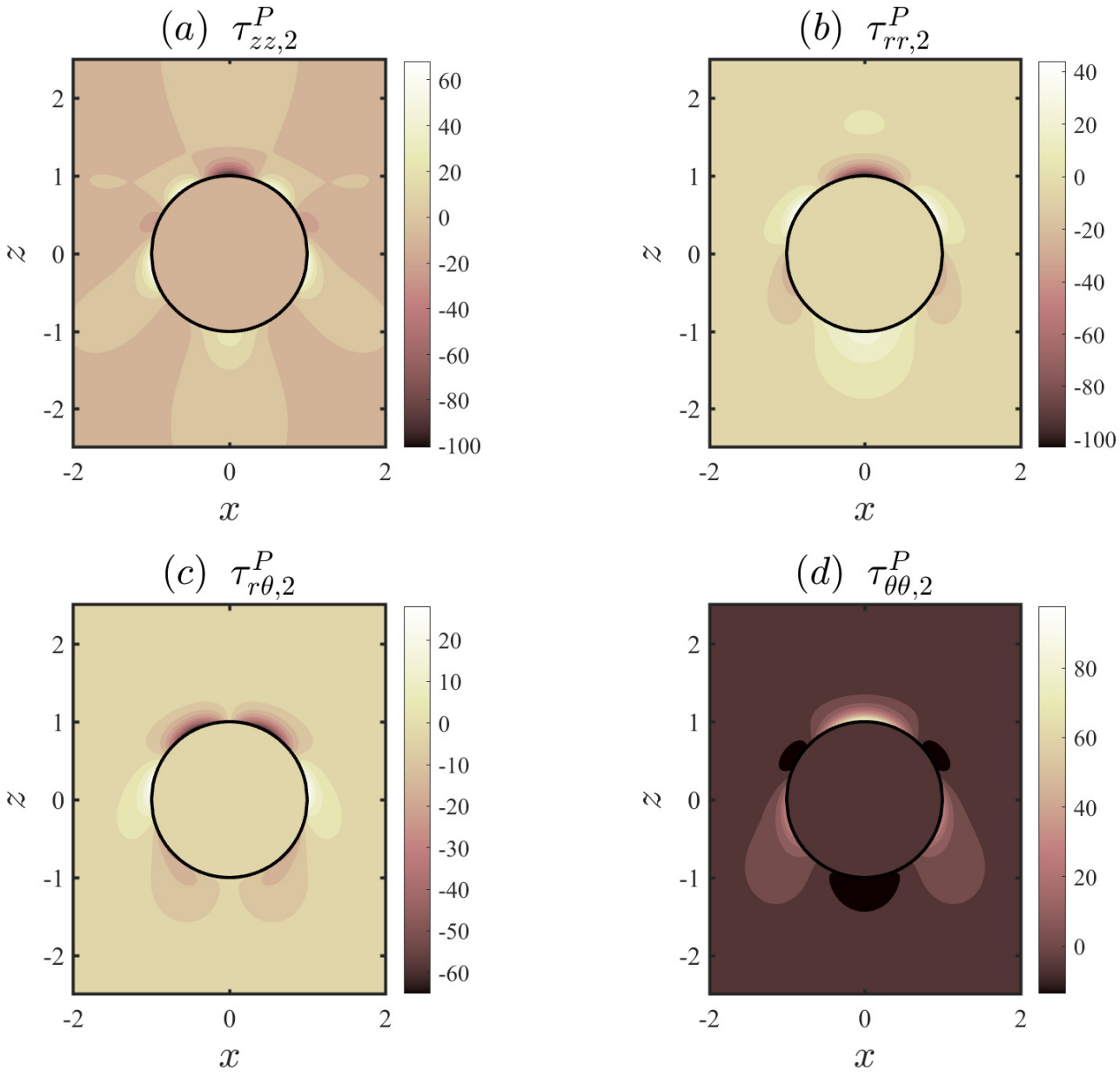

Figure S2: Contour plots of polymeric stresses ($\boldsymbol{\tau}^P$) at $O(\bar{\zeta}_0^2)$ around a particle carrying non-uniform surface charge, where $a_0 = 0.5$ and $a_1 = 1$. Other relevant parameters are: $De = 1,\ \lambda_1 = 1,\ \lambda_2 = 0.1,\ \beta = 1$. We have plotted (a) $\tau^P_{zz,2}$; (b) $\tau^P_{rr,2}$; (c) $\tau^P_{r\theta,2}$ and (d) $\tau^P_{\theta\theta,2}$.

$\boldsymbol{\tau}^P_1 = 2\left(1 - \frac{\lambda_2}{\lambda_1}\right)\mathbf{D}_1$. Hence, the $O(\bar{\zeta}_0^2)$ correction becomes:

$$\boldsymbol{\tau}^P_2 = 2\left(1 - \frac{\lambda_2}{\lambda_1}\right)\left[\mathbf{D}_2 - De\overset{\nabla}{\mathbf{D}}_1\right] \tag{S20}$$

For extensional stresses, we may further calculate the zz component as: $\tau^P_{zz,2} = \boldsymbol{\tau}^P_2 : \hat{\mathbf{e}}_z\hat{\mathbf{e}}_z$. Figure S2 depicts the contours of the four polymeric stress components at $O(\bar{\zeta}_0^2)$, namely $\tau^P_{zz,2}$ in (a), $\tau^P_{rr,2}$ in (b), $\tau^P_{r\theta,2}$ in (c) and $\tau^P_{\theta\theta,2}$ in (d), in the xz-plane, for a non-uniformly charged particle with $a_0 = 0.5$ and $a_1 = 1$. Values of other relevant parameters have been given in the caption. The $O(\bar{\zeta}_0^2)$ term is chosen, because this is the first correction to the polymeric stresses because of the fluid's viscoelastic nature. From subfigure (a), the fore-aft asymmetry because of non-uniform charge distribution is visible. Further insight on breaking of fore-aft symmetry has been provided in §4.3. Noting that the particle here is moving upwards, the normal stress

in front of it is compressive, while behind the particle, $\tau^P_{zz,2}$ is positive, indicating polymer stretching. Qualitiatively, this distribution of τ_{zz} is similar to previously reported studies in the literature [6]. Similarly, the stress components in the spherical coordinate also show fore-aft symmetry breaking. For instance from subfigure (b), one may note that rr-component of the polymeric stresses are compressive in front of the particle and extensional in nature behind it - similar to the behavior shown by the zz-component. On the other hand, the $\theta\theta$-component shows somewhat opposite behavior. This is because the flow has a "diverging" nature near the north pole, while near the south pole it is converging, which results in $\tau^P_{\theta\theta}$ being extensional at the front and compressive at the back.

References

[1] Ehud Yariv. An asymptotic derivation of the thin-debye-layer limit for electrokinetic phenomena. *Chemical Engineering Communications*, 197(1):3–17, 2009.

[2] Uddipta Ghosh, Shubhadeep Mandal, and Suman Chakraborty. Electroosmosis over charge-modulated surfaces with finite electrical double layer thicknesses: Asymptotic and numerical investigations. *Physical Review Fluids*, 2(6):064203, 2017.

[3] Robert Byron Bird, Robert C Armstrong, and Ole Hassager. *Dynamics of polymeric liquids. Vol. 1: Fluid mechanics*. 1987.

[4] John L Anderson. Effect of nonuniform zeta potential on particle movement in electric fields. *Journal of colloid and interface science*, 105(1):45–54, 1985.

[5] Gaojin Li and Donald L Koch. Electrophoresis in dilute polymer solutions. *Journal of Fluid Mechanics*, 884, 2020.

[6] Oliver G Harlen. The negative wake behind a sphere sedimenting through a viscoelastic fluid. *Journal of Non-Newtonian Fluid Mechanics*, 108(1-3):411–430, 2002.